


# Analysis of the optimal target node to reduce seizure-like discharge in networks

Luyao Yan(闫璐瑶), Honghui Zhang(张红慧), and Zhongkui Sun(孙中奎)

**Citation:**Chin. Phys. B, 2024, 33 (**5**): 058703. DOI: 10.1088/1674-1056/ad3346

**What follows is a list of articles you may be interested in**

---

## Effect of cognitive training on brain dynamics

Guiyang Lv(吕贵阳), Tianyong Xu(徐天勇), Feiyan Chen(陈飞燕), Ping Zhu(朱萍), Miao Wang(王淼), and Guoguang He(何国光)

Chin. Phys. B, 2024, 33 (**2**): 028704. DOI: 10.1088/1674-1056/ad09c8

## Astrocyte and ions metabolism during epileptogenesis: A review for modeling studies

Meng-Meng Du(独盟盟), Jia-Jia Li(李佳佳), Zhi-Xuan Yuan(袁治轩), Yong-Chen Fan(范永晨), Ying Wu(吴莹)

Chin. Phys. B, 2020, 29 (**3**): 038701. DOI: 10.1088/1674-1056/ab6961

## Cross-frequency network analysis of functional brain connectivity in temporal lobe epilepsy

Hai-Tao Yu(于海涛), Li-Hui Cai(蔡立辉), Xin-Yu Wu(武欣昱), Jiang Wang(王江), Jing Liu(刘静), Hong Zhang(张宏)

Chin. Phys. B, 2019, 28 (**4**): 048702. DOI: 10.1088/1674-1056/28/4/048702

## Effect of focused ultrasound stimulation at different ultrasonic power levels on the local field potential power spectrum

Yuan Yi (袁毅), Lu Cheng-Biao (路承彪), Li Xiao-Li (李小俚)

Chin. Phys. B, 2015, 24 (**8**): 088704. DOI: 10.1088/1674-1056/24/8/088704

## Closed-loop control of epileptiform activities in a neural population model using a proportional-derivative controller

Wang Jun-Song (王俊松), Wang Mei-Li (王美丽), Li Xiao-Li (李小俚), Ernst Niebur

Chin. Phys. B, 2015, 24 (**3**): 038701. DOI: 10.1088/1674-1056/24/3/038701

---

# Analysis of the optimal target node to reduce seizure-like discharge in networks

Luyao Yan(闫璐瑶)[1], Honghui Zhang(张红慧)[1,2,†], and Zhongkui Sun(孙中奎)[1,‡]

[1] *School of Mathematics and Statistics, Northwestern Polytechnical University, Xi'an* 710129, *China*
[2] *MIIT Key Laboratory of Dynamics and Control of Complex Systems, Xi'an* 710129, *China*

(Received 25 December 2023; revised manuscript received 23 February 2024; accepted manuscript online 13 March 2024)

Network approaches have been widely accepted to guide surgical strategy and predict outcome for epilepsy treatment. This study starts with a single oscillator to explore brain activity, using a phenomenological model capable of describing healthy and epileptic states. The ictal number of seizures decreases or remains unchanged with increasing the speed of oscillator excitability and in each seizure, there is an increasing tendency for ictal duration with respect to the speed. The underlying reason is that the strong excitability speed is conducive to reduce transition behaviors between two attractor basins. Moreover, the selection of the optimal removal node is estimated by an indicator proposed in this study. Results show that when the indicator is less than the threshold, removing the driving node is more possible to reduce seizures significantly, while the indicator exceeds the threshold, the epileptic node could be the removal one. Furthermore, the driving node is such a potential target that stimulating it is obviously effective in suppressing seizure-like activity compared to other nodes, and the propensity of seizures can be reduced 60% with the increased stimulus strength. Our results could provide new therapeutic ideas for epilepsy surgery and neuromodulation.

**Keywords:** epilepsy, driving node, epileptic node, seizure regulation

**PACS:** 87.19.le, 87.19.xm **DOI:** 10.1088/1674-1056/ad3346

## 1. Introduction

Epilepsy is a neurological disease that has developed into a public health imperative, affecting about 70 million people worldwide.[1] Due to the structural and functional disorder in the brain, neurons show pathological synchronized discharges and epilepsy seizures appear.[2,3] Recurrent seizures disturb the normal life of patients seriously. The epilepsy treatment has long been a popular issue in the medical community, and drug therapy is generally used in clinical practice. Though antiepileptic drugs are continuously developed, there are still more than 30% of patients suffering recurrent seizures after long-term treatment. For these patients, surgery and neuromodulation therapy are regarded as potential ways by which to get rid of seizures.[4,5] However, identifying resection or stimulus target directly impacts the treatment outcome. Therefore, it is particularly important to understand the mechanism of seizure generation and determine the accurate target of epilepsy therapy.

According to neuroimaging data, large-scale brain networks are widely constructed which cover structural and functional features.[6–8] Network theory approach is to simplify these features and establish mathematical models in which brain regions are considered as nodes and connections among various regions are network edges. The obtained model is able to reveal the temporal evolution of node and the topological property of network. This method has been devoted to exploring brain diseases, and epilepsy is listed among them.[9–11] Such approach has first application in researching network characteristics during epileptic seizures. Seizures have been found to depend on the network structure and pathological regions, thus changes in these two aspects can produce epilepsy.[12–15] Also, various states of the brain have corresponding topologies of functional networks, especially in pre- and post-seizures.[16] The indicators in the graph theory further show network features in seizures. Compared to healthy networks, the mean node degree of epileptic networks is higher, meaning that networks with high node degrees tend to produce epileptic dynamics and increase the incidence of seizures.[17] Healthy and epileptic brains may reflect changes in clustering coefficients, and small-world networks have higher clustering coefficients which are prone to seizures.[18] All these studies have suggested the effect of network topology on the epilepsy pathogenesis.

External perturbations can simulate surgery resection[19,20] and neuromodulation therapy,[21–23] which is helpful to develop effective treatments. In the case of epilepsy surgery, the network approach is a potential avenue to guide strategies and predict outcomes which are modeled by removing nodes or edges *in vitro*. Generally speaking, resecting key regions is a preferred way, such as epileptic focus or seizure onset zone, but it does not always result in the best surgical outcome.[24,25] In addition, the selection of removed nodes is

†Corresponding author. E-mail: haozhucy@nwpu.edu.cn
‡Corresponding author. E-mail: dynsun@126.com

© 2024 Chinese Physical Society and IOP Publishing Ltd 

likely to depend on the network structure. For example, in scale-free and rich-club networks, specific nodes should be removed which are critical for seizures, whereas in small-world networks, removing enough nodes might be effective in controlling seizures.[26] This reveals that patients may have inconsistent responses to the same surgery strategy because network connections are different, which increases the difficulty in the surgery. Therefore, it is necessary to provide a universal resection scheme which is as independent as possible from the network structure. Research[27,28] have focused on driving nodes in four-nodes networks, and compared the trend of brain network ictogenicity (BNI) which described the propensity of a network to generate seizures. Results show BNI is higher in networks that contain driving nodes and highlight a decision role of driving nodes in epilepsy networks. However, how to choose the node to be removed is still intractable, i.e., abnormal hyperexcitable nodes or important nodes in the network, and there is not yet a relatively uniform strategy.

In this context, we aim to investigate the generation of seizure-like activity and the influence of resection on epilepsy networks. The model we used is a phenological model that includes the healthy background state and epileptic state, which is a modified model of the form of the subcritical Hopf bifurcation, and offers a theoretical framework to explain the coexistence of healthy and pathological states by bifurcation analysis.[13,29] This type of model is a simplification of biophysics models, and can suggest the key feature during the seizures process and give exhaustive research on dynamics.[30,31] Based on this, Hebbink *et al*. introduced the oscillator excitability as a slow variable and considered node dynamics as a fast-slow system.[27] Noise or perturbation can induce transition behaviors between healthy and epileptic states, and a number of studies have focused on the seizure generation and effective regulation paradigms.[17,27,29] Thus, using the model to inscribe the node dynamics can achieve our research purpose. On the one hand, a comprehensive study of seizure features could be helpful to prevent epilepsy from the point of mechanisms. On the other hand, exploring common resection strategies can provide theoretical guidance for epilepsy surgery.

## 2. Model

### 2.1. Dynamical analysis for a single oscillator

Computational model is a means of gaining insight into the discharge mechanisms of neuronal systems, usually contains realistic models derived from real biological experiments and phenomenological models constructed to reveal the common property. The choice of phenomenological models to characterize large-scale networks has the advantage of being computationally small in the case where phenomenological model has an approximately match to realistic models. Here, we introduce a phenomenological model to describe transition behaviors between inter-ictal and ictal states of epilepsy. The dynamical description is as follows:[13,27,29]

$$\begin{cases} \dot{z} = z(\lambda - 1 + \mathrm{i}\omega + 2|z|^2 - |z|^4) + \alpha dW, \\ \tau\dot{\lambda} = \lambda_0 - \lambda - |z|^2, \end{cases} \tag{1}$$

where $z = x + \mathrm{i}y$ is a complex activity variable. The model has the correspondence with the known biophysics system.[32] Correspondingly, the real part $x$ is interpreted as the membrane potential of excitatory pyramidal population and the imaginary part $y$ is the membrane potential of inhibitory interneurons in the cortex. $\lambda$ is a real variable that represents the oscillator excitability and affects the balance between excitation and inhibition function. $\tau$ is the speed of oscillator excitability $\lambda$ and regulates the release of neurotransmitter. $\lambda_0$ is the excitability level and the parameter $\omega$ represents the oscillation frequency that is around 3 Hz when $\omega = 20$. The Weiner process $W$ with noise strength $\alpha$ shows the background input from other regions.

To understand the dynamical property of the oscillator, we calculate solutions of Eq. (1) and analyze the stability without the noise input $\alpha dW$. Through phase rotations $z \to \mathrm{e}^{\mathrm{i}\phi(t)}z$, $\dot{\phi(t)} = \omega$, the time evolutions of the radial and angular are $z(t) = \sqrt{\rho(t)}\,\mathrm{e}^{\mathrm{i}\phi(t)}$, $\rho(t) = |z|^2 = z\bar{z}$, and the obtained equation is given below:

$$\begin{cases} \dot{\rho} = -2\rho^3 + 4\rho^2 + 2(\lambda - 1)\rho, \\ \tau\dot{\lambda} = \lambda_0 - \lambda - \rho. \end{cases} \tag{2}$$

The solutions of Eq. (2) satisfy

$$\begin{cases} 2\rho[-\rho^2 + 2\rho + (\lambda - 1)] = 0, \\ \lambda_0 - \lambda - \rho = 0. \end{cases} \tag{3}$$

Equation (3) has three solutions: a fixed point $\rho_1 = 0$, $\lambda_1 = \lambda_0$; limit cycles $\rho_{2,3} = (1 \pm \sqrt{4\lambda_0 - 3})/2$, $\lambda_{2,3} = \lambda_0 - \rho_{2,3}$. Combing the stationary conditions

$$\frac{\partial}{\partial\rho}\left(\frac{\mathrm{d}\rho}{\mathrm{d}t}\right)\bigg|_{(\rho,\lambda)} < 0, \quad \frac{\partial}{\partial\lambda}\left(\frac{\mathrm{d}\lambda}{\mathrm{d}t}\right)\bigg|_{(\rho,\lambda)} < 0, \tag{4}$$

we further analyze properties of the solutions. For the fixed point $(\rho_1, \lambda_1)$, we get

$$\begin{aligned} \frac{\partial}{\partial\rho}\left(\frac{\mathrm{d}\rho}{\mathrm{d}t}\right)\bigg|_{(\rho_1,\lambda_1)} &= 2(\lambda_0 - 1), \\ \frac{\partial}{\partial\lambda}\left(\frac{\mathrm{d}\lambda}{\mathrm{d}t}\right)\bigg|_{(\rho_1,\lambda_1)} &= -1 < 0, \end{aligned} \tag{5}$$

suggesting that the stationary is decided by $\lambda_0$. For periodic solutions, $\rho_{2,3} > 0$ possibly establishes when $\lambda_0 > 0.75$ and two limit cycles are unstable in the region of $\lambda_0 \in (0.75, 1)$, because

$$\frac{\partial}{\partial\rho}\left(\frac{\mathrm{d}\rho}{\mathrm{d}t}\right)\bigg|_{(\rho_{2,3},\lambda_{2,3})} = -4(\lambda_0 - 1) > 0,$$

$$\frac{\partial}{\partial\lambda}\left(\frac{\mathrm{d}\lambda}{\mathrm{d}t}\right)\Big|_{(\rho_{2,3},\lambda_{2,3})} = -1 < 0. \tag{6}$$

When $\lambda_0 > 1$, $\rho_2 > 0$ and $\rho_3 < 0$. There is a stable periodic solution $(\rho_2, \lambda_2)$, satisfying

$$\begin{aligned}\frac{\partial}{\partial\rho}\left(\frac{\mathrm{d}\rho}{\mathrm{d}t}\right)\Big|_{(\rho_2,\lambda_2)} &= -4(\lambda_0 - 1) < 0,\\ \frac{\partial}{\partial\lambda}\left(\frac{\mathrm{d}\lambda}{\mathrm{d}t}\right)\Big|_{(\rho_2,\lambda_2)} &= -1 < 0.\end{aligned} \tag{7}$$

As a whole, the solutions are roughly classified in the light of $\lambda_0$

(i) $\lambda_0 \in (0, 0.75)$, stable fixed point;

(ii) $\lambda_0 \in (0.75, 1)$, stable fixed point and unstable limit cycle;

(iii) $\lambda_0 \in (1, 2)$, unstable fixed point and stable limit cycle.

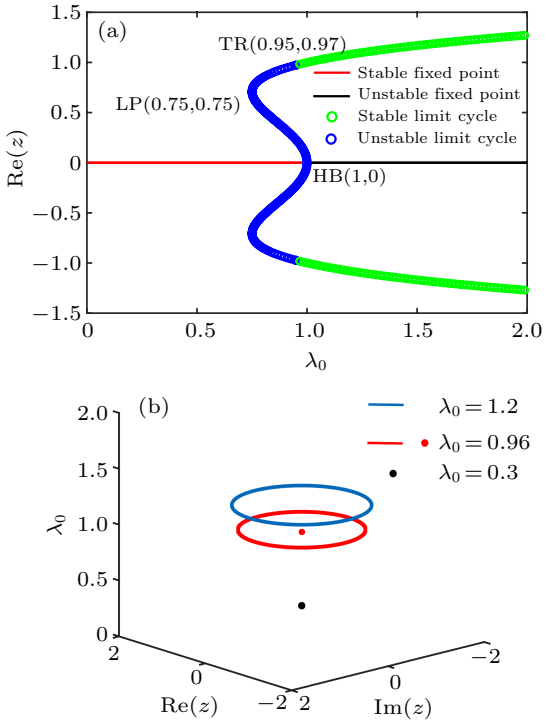



**Fig. 1.** (a) Dynamical bifurcation diagram with respect to the excitability level $\lambda_0$. The red and black lines represent stable and unstable fixed points, green and blue circles are stable and unstable limit cycles. There are three bifurcations: fold limit cycle bifurcation (LP), torus bifurcation (TR), and Hopf bifurcation (HB). (b) Phase diagram in (Re($z$), Im($z$), $\lambda_0$). The red dots are fixed points and blue circles are limit cycles with $\lambda_0 = 0.3, 0.96, 1.2$. The stable fixed point and limit cycle coexist in the region $\lambda_0 \in (0.95, 1)$.

In the meanwhile, figure 1(a) presents a bifurcation diagram with respect to the excitability level $\lambda_0$, illustrating solutions of the system by software XPP-AUTO. The red and black lines represent stable and unstable fixed points, otherwise, green and blue circles are stable and unstable limit cycles. There is a stable fixed point when $\lambda_0 < 0.75$, and the system presents background state. Next, unstable limit cycles arise from fold limit cycle bifurcation (LP) with $\lambda_0 = 0.75$, and the stable basin is still generated by the fixed point. After the Hopf bifurcation (HB) with $\lambda_0 = 1$, the stable solution is the limit cycle, thus the system shows oscillation activity. In addition, a complex limit cycle bifurcation, torus bifurcation (TR), is found numerically which induces a bistable region in $\lambda_0 \in (0.95, 1)$. In this region, the stable fixed point and limit cycle coexist as shown in Fig. 1(b) and the final state depends on initial conditions.

### 2.2. Dynamical network model and measures

To explore the effect of network topology on epileptic seizures, we apply a coupled network where each node is consisted of the phenomenological model:

$$\begin{cases} \dot{z_k} = z_k(\lambda_k - 1 + \mathrm{i}\omega + 2|z_k|^2 - |z_k|^4) \\ \qquad + \dfrac{\beta}{N}\displaystyle\sum_{j=1}^{N} A_{jk}(z_j - z_k) + \alpha dW_k, \\ \tau\dot{\lambda_k} = \lambda_{k0} - \lambda_k - |z_k|^2. \end{cases} \tag{8}$$

Here, equation (8) describes the dynamics of node $k$, and $N$ is the total number of nodes. The adjacency matrix $A$ is defined that, if node $j$ has a connection with node $k$, then $A_{jk} = 1$, otherwise $A_{jk} = 0$. In the network, diffusive coupling is regarded as the connectivity method that is linear and proportional to the difference between states of two nodes with the same strength $\beta$.

The following measures quantify the seizure of each node and network. The first one is seizure rate (SZ), calculating the rate of ictal time in all simulations:

$$\mathrm{SZ}_k = \frac{t_{\mathrm{SZ}}^k}{T}, \tag{9}$$

where $t_{\mathrm{SZ}}^k$ devotes to be the time being in the ictal state of node $k$, and $T$ is the simulation time. This indicator reflects the seizure event of each node and the contribution to the overall network. To assess the seizure dynamics in networks, quite a few studies have used the second one, brain network ictogenicity (BNI).[17,19,28,33] The concept of BNI corresponds to the average time that each node spends in the ictal state, which is regulated by

$$\mathrm{BNI} = \frac{1}{N}\sum_k \frac{t_{\mathrm{SZ}}^k}{T}. \tag{10}$$

BNI characterizes the propensity that a network generates seizure-like activity, and the network is in the ictal state for a long time which causes BNI to be high. For a specific network, we aim to reduce BNI so that the network has a weaker capacity to generate seizure-like discharges. Here, we consider the coupling strength $\beta$ in a wide range, instead of restricting it to be fixed values, and the BNI is averaged over different values involving weak and strong couplings.

## 3. Results

### 3.1. Ictal number and duration are associated with the speed of oscillator excitability

An important output of the model Re($z$), i.e. PY, is used to simulate the EEG activity as figure 2(a) shows. The activity around the stable fixed point with a tiny amplitude is the inter-ictal state and the oscillation with high amplitude represents ictal state. The noise can induce transition behaviors between two states and change the oscillator excitability $\lambda$. Specifically, when the noise forces the system to display ictal activity, the oscillator excitability $\lambda$ decreases from the initial excitability level $\lambda_0 = 0.7$. When the transition to inter-ictal state happens, $\lambda$ returns to the original level $\lambda_0$, as presented in Fig. 2(b). Thus, the excitation–inhibition balance is disrupted because the oscillator excitability falls below the basic level, which generates the seizure event. It is worth pointing out that the system has a stable fixed point when $\lambda_0 = 0.7$ (Fig. 1(a)), while due to the presence of noise, transition behaviors have occurred, indicating that the system also has a limit cycle (Fig. 2(a)). To further confirm, figure 2(c) shows that there does exist a bistable region consisting of the fixed point and limit cycle, and the trajectory can jump between them with $\alpha = 0.1$. This illustrates that the bifurcation phenomenon is qualitatively altered by the noise perturbation.

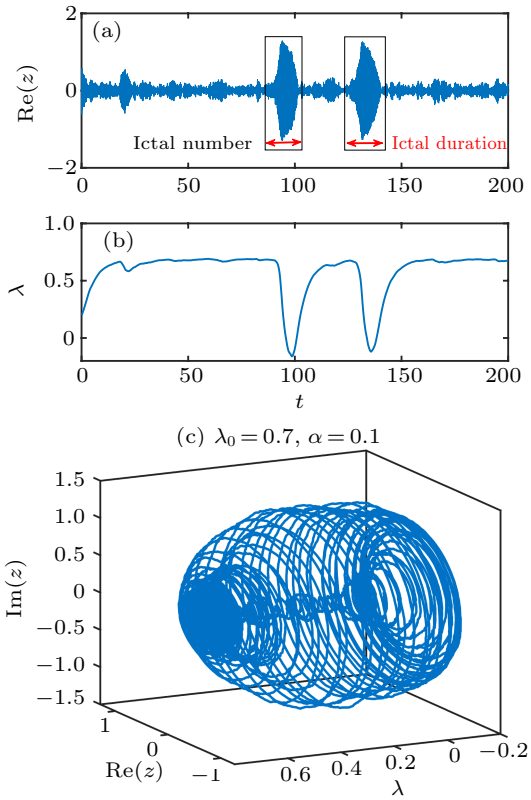



**Fig. 2.** (a) Time series of Re($z$)–$t$, ictal number = 2, ictal duration ≈ 5 s. (b) Time series of $\lambda$–$t$. (c) Phase diagram when $\lambda_0 = 0.7$, $\alpha = 0.1$, and the bifurcation phenomenon is qualitatively altered by the noise perturbation.

Recurrent seizures are bound to be harmful to patients, so it is necessary to recognize potential inducements, which is helpful to prevent seizures. We firstly concern the ictal number which refers to how many times seizures occur in a period of time, for example, ictal number is two in Fig. 2(a). Figure 3 describes how ictal number links to the speed of oscillator excitability $\tau$ within 500 s, when excitability level $\lambda_0$ and noise strength $\alpha$ are fixed, respectively. Taken as a whole, the ictal number decreases progressively or remains unchanged with respect to the speed of oscillator excitability $\tau$. This is because with increasing the speed of oscillator excitability, changes in the oscillator excitability occur relatively slowly. Nonetheless, the effect of noise on the ictal number is clearly visible in Fig. 3(a) with $\lambda_0 = 0.7$. When $\alpha = 0.05$, 0.08, the ictal number is zero, thus the system remains in the healthy state though there is a weak perturbation. As $\alpha = 0.1$, the noise induces transition behaviors and the ictal number is non-zero, which happens in a bistable region with $\lambda_0 = 0.7$. When $\alpha$ proceeds to change, the ictal number has increased for the same value of $\tau$, suggesting the system is easier to arrive the limit cycle basin under strong noise perturbation. A similar effect of excitability level $\lambda_0$ on the ictal number is observed in Fig. 3(b) at a given noise strength $\alpha = 0.1$. For the same $\tau$, the ictal number increases because the system is more active in two basins when $\lambda_0$ is larger.

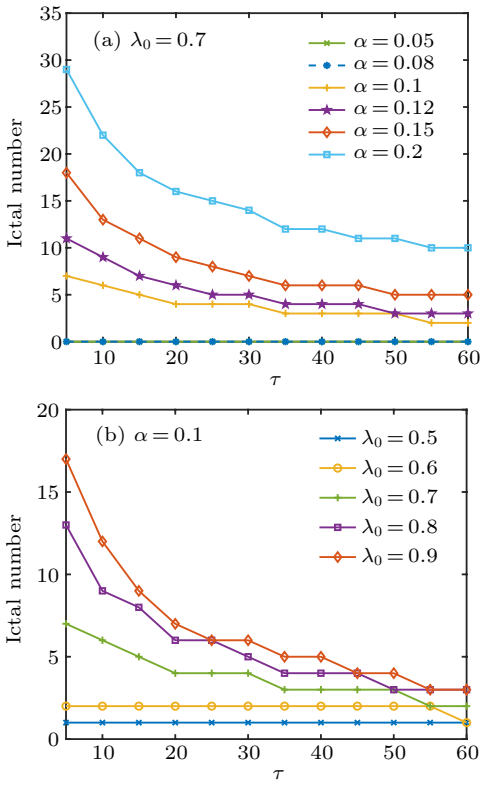



**Fig. 3.** Ictal number changes with respect to the speed of oscillator excitability $\tau$. Taken as a whole, the ictal number decreases progressively or remains unchanged with respect to $\tau$. (a) When the noise strength $\alpha$ proceeds to change, the ictal number increases for the same $\tau$, indicating the system is easier to arrive the limit cycle basin under strong noise perturbation, given $\lambda_0 = 0.7$. (b) The excitability level $\lambda_0$ also has a similar effect on the ictal number, given $\alpha = 0.1$. For the same $\tau$, the ictal number increases because the system is more active in two basins when $\lambda_0$ is larger.

In each seizure event, the ictal duration is determined by the slow dynamics and its speed, but the exact relationship is still unclear.[27] Based upon, we find that there is an increasing trend of the ictal duration when the speed of oscillator excitability $\tau$ changes as figure 4 shows. To be specific, the larger $\alpha$, the smaller duration is (Fig. 4(a)). It is much more frequent that the system transits between two states under the stronger noise, which causes the duration in a specific state is temporary. Different from the effect of $\alpha$, the ictal duration also increases when $\lambda_0$ is increased under the same $\tau$, indicating that the active oscillator is prone to keep in the limit cycle basin for a long time. Therefore, our results suggest that the ictal duration can be predicted according to the speed of oscillator excitability.

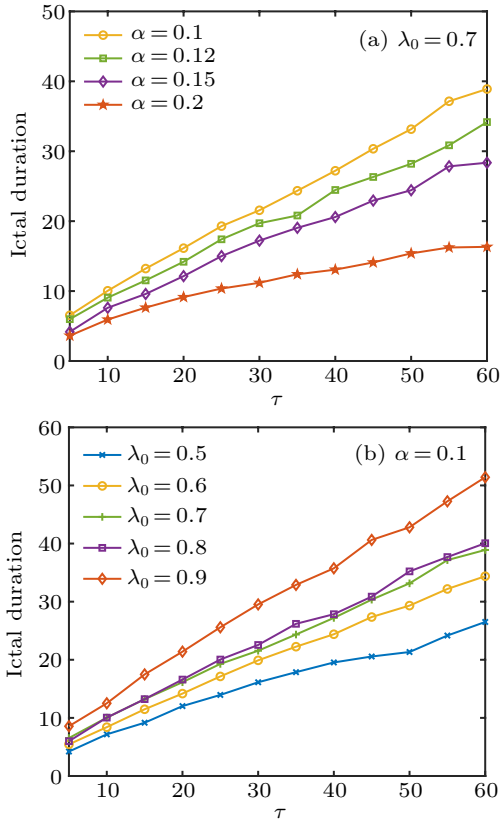



**Fig. 4.** Ictal duration changes with respect to the speed of oscillator excitability $\tau$. There is an increasing trend of the ictal duration along with the speed $\tau$. (a) Given $\lambda_0 = 0.7$, the larger $\alpha$, the smaller duration is. (b) Given $\alpha = 0.1$, the ictal duration also increases when $\lambda_0$ is increased under the same $\tau$. Our results suggest that the ictal duration can be predicted according to the speed of oscillator excitability.

### 3.2. Removing critical node is effective for seizure regulation

Changes in the network structure do affect the propensity of seizures, and surgery treatment aims to remove the key issue to prevent recurrence seizures. Removing nodes and edges can simulate the surgery process from a computational modeling perspective, and how to identify the target node has caught increasing focus. In this study, we assess two types of important nodes in epilepsy networks. The first one is serious epileptic node (EN) which has the maximum of SZ, and removing EN is a preferred choice in the traditional surgery for epilepsy treatment. Another one is driving node (DN), of which the in-degree is zero. As examples, figure 5 shows three four-node networks with different edges and the DN is marked by red in each network. This type of node plays a decisive role in the network, for example, if the node displays oscillation activity and other nodes do not, all nodes will show synchronous oscillation activity eventually. Therefore, it is worthy of further investigation on which types of nodes to be removed for seizure regulation.

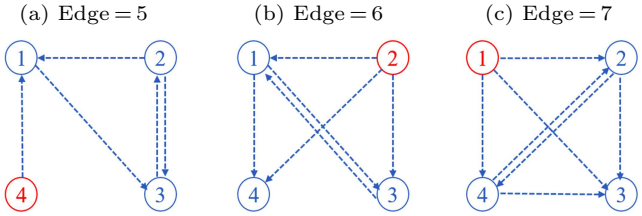



**Fig. 5.** Four-node networks have a single driving node which is marked by red: (a) edge = 5, (b) edge = 6, (c) edge = 7; the following investigation is based on the network (b).

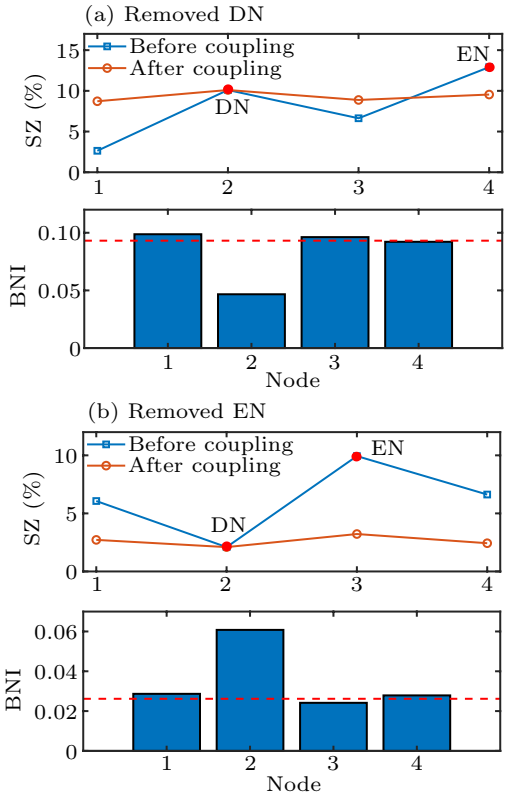



**Fig. 6.** Two cases about node removal are shown, one is DN and the other is EN. (a) Node 4 is marked as the EN, the DN (node 2) has a lower value of SZ before coupling (blue line). BNI of the network is close to 0.1, depicted by the red dash line, and the blue bar chart shows BNI of the remained connected network. BNI is the minimal after removing DN, while has a little variation even increase after removing other nodes. Thus, DN is the primary target and other nodes are ineffective. (b) By contrast, removing EN can reduce BNI while removing other nodes cannot.

We start with a small scale network with four-nodes, in which there are 66 networks with a single DN. To compare the

propensity of seizures after removing nodes, we select a specific network (Fig. 5(b)) where node 2 is a DN and the following investigation is based on this network. Instead of fixing the value of coupling strength $\beta$, we vary it from weak to strong coupling, and calculate the average value of BNI. In each simulation, the randomly generated noise is different, so BNI of the network and the node marked as EN will also be different. Two cases about node removal are shown in Fig. 6, one is DN and the other is EN. In the upper subfigure of Fig. 6(a) where node 4 is marked as the EN, the DN (node 2) has a lower value of SZ before coupling (blue line), as well as the SZ of each node is almost equal after coupling (orange line). BNI of the network is close to 0.1, depicted by the red dash line in the lower subfigure of Fig. 6(a). We try to remove each node to reduce BNI, and the blue bar chart shows BNI of the remained connected network. Interestingly, BNI is the minimal after removing DN, while BNI has a little variation even increase after removing other nodes. Thus, DN is the primary target and other nodes are ineffective. In another situation, as figure 6(b) displays, we find that removing EN can reduce BNI while removing other nodes can not. The reason lies in the apparent difference in $SZ_{EN}$ and $SZ_{DN}$ in which DN is almost in the non-seizure state. The results reveal that the selection of removal nodes not only depends on the initial seizure condition, but also associates with the node position in the network.

According to our simulation, DN and EN both may be the removal target, but how to select is still unclear. After 1000 simulations, we classify the outcome into two categories. One part is the case where the removal of DN is effective (Figs. 7(a) and 7(b)) and occupies relatively great proportion, in which the condition $SZ_{DN} = SZ_{EN}$ is omitted. According to Fig. 7(a), we find that $SZ_{EN}$ (red dots) and $SZ_{DN}$ (blue dots) mix together and there is no sharp line separating $SZ_{DN}$ from $SZ_{EN}$, which is also demonstrated by counting the occurrence of $SZ_{EN}$ and $SZ_{DN}$ as shown in Fig. 7(b). In the other case, the target node of removing is EN. $SZ_{DN}$ is obviously lower than $SZ_{EN}$, and there is a distinct boundary between the two in Figs. 7(c) and 7(d). In order to distinguish the two situations more clearly, we propose an indicator $\Delta P = \mathrm{Pro}(SZ_{EN}) - \mathrm{Pro}(SZ_{DN})$, that is the difference between the proportion of $SZ_{EN}$ and $SZ_{DN}$ in the network. We find that there is a threshold, roughly equivalent to 0.2 in our simulation, that can separate two kinds of outcome when the edge is 6 in Fig. 8(b). When $\Delta P$ is less than the threshold, DN is probably considered as the removal node, and when $\Delta P$ is greater than the threshold, the target node is more possible to be EN. In the network, the coupling term is proportional to the difference between node states and attracts the receiving node to move towards the delivering node. Thus, the DN exerts attractive function to other nodes and is not influenced by others. When this type of nodes is removed, the coupling effect is weakened and the propensity of seizures is reduced to a greater extent. In summary, when DN and EN have similar seizures, the DN plays a dominant role and removing it can control seizures in the network.

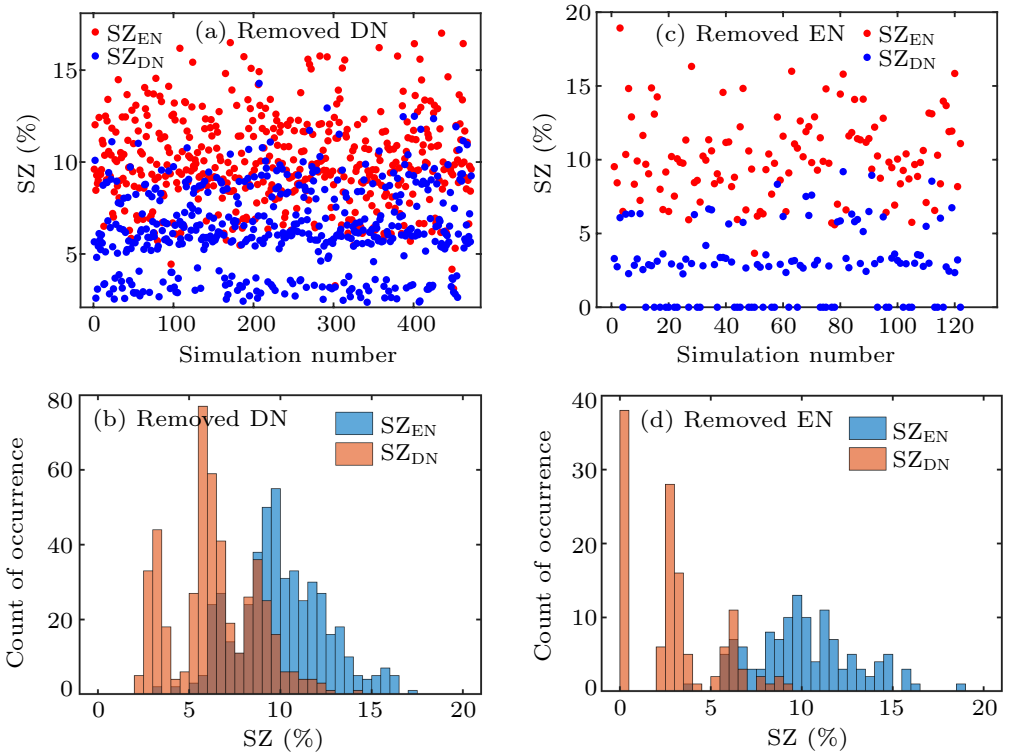



**Fig. 7.** (a) Seizure rates (SZ) of EN and DN, (b) count of occurrence of $SZ_{DN}$ and $SZ_{EN}$ in simulations when the removal of DN is effective. $SZ_{DN}$ and $SZ_{EN}$ mix together and there is no sharp line separating $SZ_{DN}$ from $SZ_{EN}$. (c) SZ of EN and DN, (d) count of occurrence of $SZ_{DN}$ and $SZ_{EN}$ when the target node of removing is EN. $SZ_{DN}$ is obviously lower than $SZ_{EN}$ and there is a distinct boundary between the two.

Without loss of generality, we verify the above conclusions in all 66 four-node networks having a single DN. These networks are divided into seven groups by edges, in which the minimal edge is three and the maximal is nine. The number of simulated networks (SN) under each edge is recorded in Fig. 8(a). In each group, we clarify the outcomes and calculate the rates that removing DN is effective in different network structures. Then we show a statistical result in each group, and find the rate has a growing tendency. As well, as figure 8(b) displays, for a specific network in each group, when $\Delta P$ is less than the threshold, removing DN is more possible to reduce the propensity of seizures significantly, while $\Delta P$ exceeds the threshold, EN is likely a preferred target. Meanwhile, the difference between the proportion of $SZ_{EN}$ and $SZ_{DN}$ is a potential indicator, which may assist in determining the optimal node to be removed. Thus, our result also holds true and has robustness to the network structure.

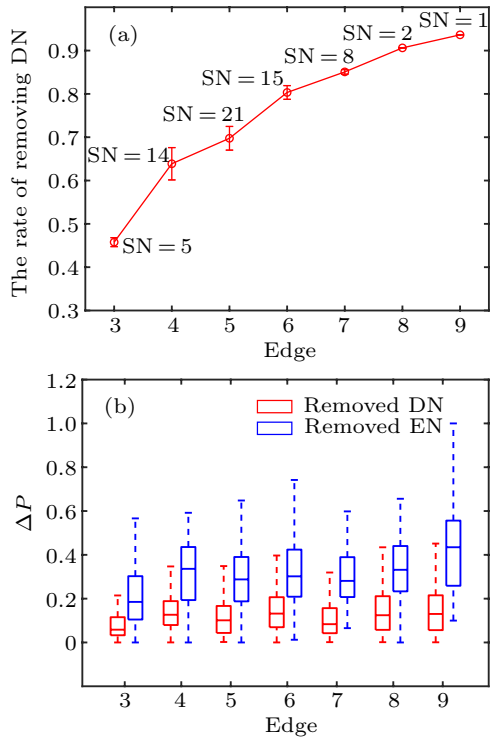



**Fig. 8.** Statistical results under different network structures. (a) In each group, SN refers to the number of simulated networks, and the rate that removing DN is effective has a growing tendency. (b) For a specific network in each group, the $\Delta P = \mathrm{Pro}(SZ_{EN}) - \mathrm{Pro}(SZ_{DN})$ is less than the threshold, DN is probably considered as the removal node, and when $\Delta P$ is greater than the threshold, the target node is more possible to be EN.

### 3.3. Stimulating driving node is another way for seizure regulation

In addition to the surgery treatment, neuromodulation therapy has been a widely applicable method in epilepsy regulation, of which, a representative one is deep brain stimulation (DBS). The rectangular pulse is the common waveform not only in the experiments but also in clinical cases, and there are lots of stimulus parameters that can be adjusted to achieve a great control effect. To compare the stimulus outcome, we introduce an indicator, $NI_k$, which is defined as given below:

$$NI_k = \frac{BNI_k - BNI_0}{BNI_0}. \tag{11}$$

$BNI_0$ is the initial BNI of the network, and $BNI_k$ is the value after stimulating the node $k$. $NI_k < 0$ means stimulating the node $k$ can reduce BNI of the network, while $NI_k > 0$ illustrates that stimulating the node $k$ induces more seizures.

In this subsection, we still choose the network in Fig. 5(b) and perform the rectangular pulse on each node to examine whether external DBS can reduce BNI of the network. When detecting the seizure event of the node $k$, the stimulation is just applied on this node, which is paused when the seizure disappears. Moreover, the stimulus strength $K$ is another factor to change. Figure 9 shows the NI–$K$ curves when stimulating different nodes. Specifically, stimulating the node 2 which is the DN in the network notably reduces seizures for all strengths $K$ due to $NI_2 < 0$ (orange line). On the contrary, the purple line depicts $NI_4 > 0$ and the stimulation induces more seizure-like discharges when the node 4 is the stimulus target. For the node 1 (blue line) and the node 3 (yellow line), the control effects are comparable. It is worthy noting that $NI_2$ is monotonically decreasing with respect to the stimulus strength $K$, illustrating that the control effect is continuously improved. Such observation reveals in a way that the DN is obviously the best target for DBS.

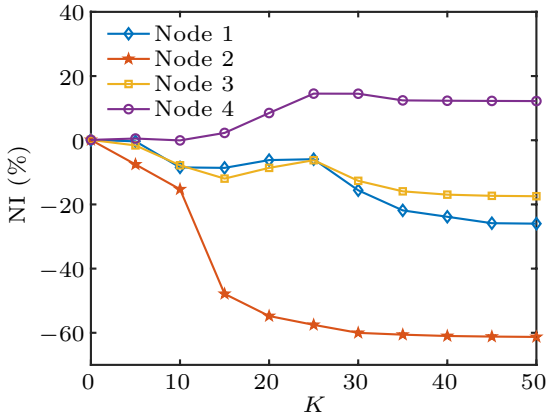



**Fig. 9.** NI–$K$ curves when stimulate different nodes. Stimulating the node 2 which is the DN in the network notably reduces seizures for all strengths $K$ due to $NI_2 < 0$ (orange line). On the contrary, the purple line depicts $NI_4 > 0$ and the stimulation induces more seizure-like discharges when the node 4 is the stimulus target. For the node 1 (blue line) and the node 3 (yellow line), the control effects are comparable.

As examples, we show the time series of each node under two different cases where $K = 10$ (Fig. 10(a)) and $K = 20$ (Fig. 10(b)), and the stimulus target is the node 2. In Fig. 10, seizure discharges occur in the first 200 s, and the same seizure is reproduced in 200 s–400 s. When detecting a seizure event in 200 s–400 s, we apply the stimulation immediately (red line). We find that oscillation activities are partially reduced with a small strength $K = 10$ and seizure-like discharges disappear for the most in the network with a large one $K = 20$.

That is, the external stimulation with large strength can effectively release seizures when the DN is the stimulus target, which might provide a possible treatment strategy for epilepsy.

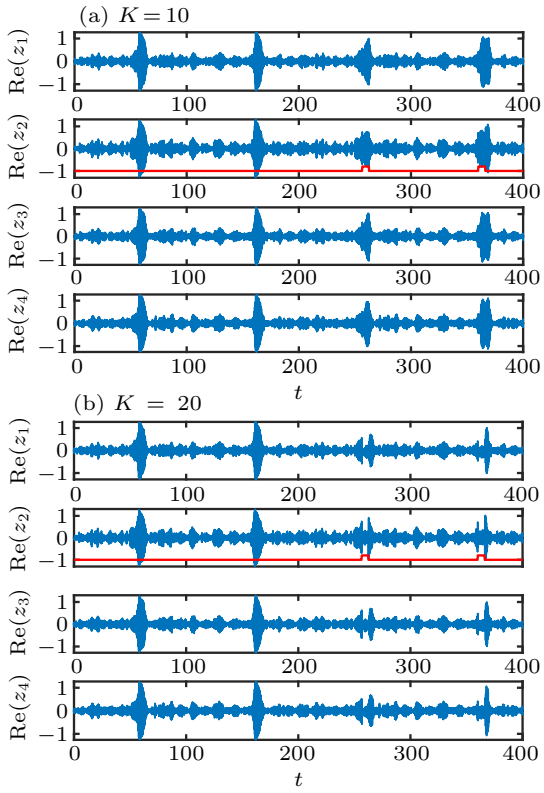



**Fig. 10.** Time series of each node when the stimulus target is the node 2. Seizures occur in the first 200 s, and the same seizure is reproduced in 200 s–400 s. When detecting a seizure event in 200 s–400 s, the stimulation is applied immediately (red line). (a) Oscillation activities are partially reduced with a small strength $K = 10$. (b) Seizure-like discharges disappear for the most in the network with a large one $K = 20$.

## 4. Discussion and conclusion

In this context, we used a phenomenological model to understand the seizure trend by exploring brain activity. For an individual oscillator, both theoretical and numerical analyses demonstrated that bifurcation phenomena changed the solution stability, and limit cycle and fixed point coexisted in a specific region, which revealed the model was capable of describing transition behaviors between healthy and epileptic states. To find potential features of seizure, effects of the speed of oscillator excitability, excitability level and noise strength were discussed, respectively. When either excitability level or noise strength was fixed, the ictal number of seizures decreased or remained unchanged with respect to the speed of oscillator excitability (Fig. 3). This was because the increment in the speed of oscillator excitability made oscillator excitability change relatively slowly, and transitions between the two attractors had been difficult. The ictal duration in each seizure showed an increasing tendency, which might provide theoretical support for epilepsy prediction (Fig. 4).

Although previous studies have stressed the importance of driving node and hyperexcitable node,[27,28] there is still no clear removal strategy during epilepsy surgery. We try to bridge this gap and further estimate how to select nodes to be removed to control seizures in the network. We proposed an indicator $\Delta P$ that was the difference between the proportion of $SZ_{EN}$ and $SZ_{DN}$, and compared two strategies for resecting nodes, one of which was DN and the other was EN. Results showed that removing DN significantly reduced BNI when $\Delta P$ was lower than the threshold, which occupied a large proportion in all simulations (Fig. 7). When $\Delta P$ was larger than the threshold, removing EN might be more effective when $\Delta P$ was larger than the threshold. In all four-node networks containing a single DN, the above conclusions were further confirmed and suggested that DN played a decision role in the epileptic network, which were independent of the network structure (Fig. 8). Analogizing DN to active regions in the brain, this might explain the phenomenon that patients do not completely achieve seizure-freedom despite the epileptic focus has been resected.[34,35] Generally, the region with serious seizures, first and foremost, draws the attention in clinic, but it may not trigger seizures within the network. By way of comparison, the active region is retained in the surgery, which could propagate the pathological activity to surrounding regions. Furthermore, stimulating DN was superior to other nodes in deep brain stimulation, as well the regulation effect was improved with the increased stimulus strength (Fig. 9), therefore, the DN was also a potential target in the neuromodulation. In conclusion, not only in the surgery, but also in the neuromodulation, identifying active regions is crucial to choose regulation strategy.

More than that, it should point out the boundedness of this study and the orientation in the future research. First, we observed an approximately linear relationship between the ictal duration and the speed of oscillator excitability, which was limited to an oversimplified model. The exact relationship should be further verified with a complex physiologically model.[36–38] Second, high-order interaction is widespread in the network, which originates from the regulation role of astrocyte and glial cells in the neural system.[39–41] A number of studies have focused on the synchronization behaviors underlying higher-order interactions. For example, high-order interaction can lead to the traveling-wave propagation,[42] enhance the neuronal synchronization,[43] and realize the optimal control on synchronization.[44] These works are of great interest for avoiding pathological synchronization, which highlights considering the higher-order interaction in epilepsy networks is a significant direction in future researches. In addition, our study is based on four-node networks and shows the robustness to the network structure. However, the brain is extremely complex, which hints to expand obtained results in a large-scale network. This study might provide novel insights into the mechanism and therapy on epilepsy. Meanwhile, it will be more meaningful to apply the current results in combination

with the functional network.

## Acknowledgement

Project supported by the National Natural Science Foundation of China (Grant Nos. 12072265, 12272295, and 11972288).

## References

[1] Thijs R D, Surges R, O'Brien T J and Sander J W 2019 *Lancet* **393** 689
[2] Seeley W W, Crawford R K, Zhou J, Miller B L and Greicius M D 2009 *Neuron* **62** 42
[3] Kramer M A and Cash S S 2012 *Neuroscientist* **18** 360
[4] Kwan P, Brodie and Martin J 2000 *New England Journal of Medicine* **342** 314
[5] Laxer K D, Trinka E, Hirsch L J, Cendes F, Langfitt J, Delanty N, Resnick T and Benbadis S R 2014 *Epilepsy Behav.* **37** 59
[6] Suk H, Wee C Y, Lee S W and Shen D 2016 *NeuroImage* **129** 292
[7] Breakspear M 2017 *Nat. Neurosci.* **20** 340
[8] Yu H T, Cai L H, Wu X Y, Wang J, Liu J and Zhang H 2019 *Chin. Phys. B* **28** 048702
[9] Englot D J, Hinkley L B, Kort N S, *et al.* 2015 *Brain* **138** 2249
[10] Proix T, Bartolomei F, Guye M and Jirsa V K 2017 *Brain* **140** 641
[11] Jirsa V K, Proix T, Perdikis D, *et al.* 2017 *Neuroimage* **145** 377
[12] Terry J R, Benjamin O and Richardson M P 2012 *Epilepsia* **53** e166
[13] Benjamin O, Fitzgerald T H, Ashwin P, Tsaneva A K, Chowdhury F, Richardson M P and Terry J R 2012 *J. Math. Neurosci.* **2** 1
[14] Taylor P N, Kaiser M and Dauwels J 2014 *J. Neurosci. Methods* **236** 51
[15] Fornito A, Zalesky A and Breakspear M 2015 *Nat. Rev. Neurosci.* **16** 159
[16] Lopes M A, Richardson M P, Abela E, Rummel C, Schindler K, Goodfellow M and Terry J R 2018 *Front. Neurol.* **9** 98
[17] Petkov G, Goodfellow M, Richardson M P and Terry J R 2014 *Front. Neurol.* **5** 261
[18] Gerster M, Berner R, Sawicki J, Zakharova A, Škoch A, Hlinka J, Lehnertz K and Schöll E 2020 *Chaos* **30** 123130
[19] Goodfellow M, Rummel C, Abela E, Richardson M P, Schindler K and Terry J R 2016 *Sci. Rep.* **6** 29215
[20] Sip V, Hashemi M, Vattikonda A N, Woodman M M, Wang H, Scholly J, Medina V S, Guye M, Bartolomei F and Jirsa V K 2021 *PLoS Comput. Biol.* **17** e1008689
[21] Lüttjohann A, Schoffelen J M and Van L G 2014 *Neurobiol. Dis.* **70** 127
[22] Stam C J 2014 *Nat. Rev. Neurosci.* **15** 683
[23] Wang J S, Wang M L and Li X L 2015 *Chin. Phys. B* **24** 038701
[24] Bertram E H 2009 *Epilepsy Behav.* **14** 32
[25] Thom M, Mathern G W, Cross J H and Bertram E H 2010 *Ann. Neurol.* **68** 424
[26] Lopes M A, Richardson M P, Abela E, Rummel C, Schindler K, Goodfellow M and Terry J R 2017 *PLoS Comput. Biol.* **13** e1005637
[27] Hebbink J, Meijer H, Huiskamp G, Van Gils S and Leijten F 2017 *Epilepsia* **58** e147
[28] Junges L, Woldman W, Benjamin O J and Terry J R 2020 *Chaos* **30** 113106
[29] Kalitzin S N, Velis D N and Lopes da Silva F 2010 *Epilepsy Behav.* **17** 310
[30] Yang C Z, Liu Z L, Wang Q S, Wang Q Y, Liu Z and Luan G M 2021 *Nonlinear Dyn.* **104** 1901
[31] Depannemaecker D, Ezzati A, Wang H F, Jirsa V and Bernard C 2023 *Neurobiol Dis.* **182** 106131
[32] Koppert M, Kalitzin S N, Velis D N, Lopes da Silva F and Viergever M A 2014 *Int. J. Neural Syst.* **24** 1430004
[33] Lopes M A, Junges L, Woldman W, Goodfellow M and Terry J R 2020 *Front. Neurol.* **11** 74
[34] Spencer S S 2002 *Epilepsia* **43** 219
[35] Lam A D, Zepeda R, Cole A J and Cash S S 2016 *Brain* **139** 2679
[36] Wendling F, Bartolomei F, Bellanger J J and Chauvel P 2002 *Eur. J. Neurosci.* **15** 1499
[37] Deco G, Jirsa V K, Robinson P A, Breakspear M and Friston K 2008 *PLoS Comput. Biol.* **4** e1000092
[38] Taylor P N, Wang Y, Goodfellow M, Dauwels J, Moeller F, Stephani U and Baier G 2014 *PLoS One* **9** e114316
[39] Fellin T, Pascual O, Gobbo S, Pozzan T, Haydon P G and Carmignoto G 2004 *Neuron* **43** 729
[40] Perea G, Navarrete M and Araque A 2009 *Trends. Neurosci.* **32** 421
[41] Allen N J and Barres B A 2009 *Nature* **457** 675
[42] Tlaie A, Leyva I and Sendiña-Nadal I 2019 *Phys. Rev. E* **100** 052305
[43] Anwar M S and Ghosh D 2023 *Chaos* **33** 073111
[44] Tang Y, Shi D H and Lü L Y 2022 *Commun. Phys.* **5** 96